

Identification of the True Product of the Urate Oxidase Reaction

Kalju Kahn, Peter Serfozo, and Peter A. Tipton*

Contribution from the Department of Biochemistry, University of Missouri—Columbia, Columbia, Missouri 65211

Received February 4, 1997[⊗]

Abstract: The O₂-dependent oxidation of urate catalyzed by urate oxidase has been examined in order to identify the immediate product of the enzymatic reaction. Specifically labeled [¹³C]urates were utilized as substrates, and the time courses were monitored by ¹³C NMR. On the basis of chemical shift values and ¹⁸O labeling, the product of the reaction was identified as 5-hydroxyisourate. This identification was substantiated by calculation of the ¹³C NMR spectrum of 5-hydroxyisourate using *ab initio* density functional theory methods. The predominant tautomers of urate and allantoin in aqueous solution were identified from ¹³C NMR titration data; the ionization behavior of urate and 5-hydroxyisourate were also examined by computational methods. The nonenzymatic pathway for production of allantoin from 5-hydroxyisourate was delineated; the reaction proceeds by the hydrolysis of the N1–C6 bond, followed by an unusual 1,2-carboxylate shift and decarboxylation to form allantoin.

Introduction

Urate oxidase (EC 1.7.3.3) catalyzes the oxidation of urate with concomitant reduction of molecular oxygen to hydrogen peroxide. The chemical mechanism of urate oxidation is not well understood, largely because the true product of the enzymatic reaction and the cofactor content of the enzyme have long remained undefined. Some urate oxidases (e.g., the porcine enzyme) have been reported to contain copper, although it has always been found in substoichiometric amounts.¹ Enzymes from bovine liver,² bacteria,³ and fungi⁴ do not contain copper. Soybean urate oxidase is also devoid of copper, other transition metals, and common redox cofactors,⁵ thus presenting a mechanistically intriguing problem of how triplet oxygen is activated to react with the singlet urate molecule.

The exact nature of the reaction catalyzed by urate oxidase has been the subject of extensive experimental investigations. Although allantoin (**6**) is the ultimate product that forms from the oxidation of urate (**1**), the available experimental evidence suggests that urate is oxidized by the enzyme to a metastable compound which decomposes into allantoin nonenzymatically (Scheme 1). The other reaction products are hydrogen peroxide and CO₂, which is derived from C6 of urate.⁶ The pathway for conversion of urate to allantoin has been the subject of numerous studies in the past 50 years.⁷ Much of the evidence from early studies indicated that the product was a symmetrical species. When urate was labeled with ¹⁴C at C2 and converted to allantoin enzymatically, the label was found to be distributed between C2 and C7 of allantoin.⁸ Similarly, it was observed that the *in vivo* reaction with [1,3-¹⁵N₂]urate yielded allantoin in which the isotopic labels were equally distributed between

the hydantoin portion of the product and the ureido group.⁹ These observations gave rise to the suggestion that **2** is the true product of the enzymatic reaction. The observation that the primary product is optically active challenged this model, and **3** and **4** were suggested as possible candidates for the true product.¹⁰ An alternative hypothesis was put forth by Modric et al.¹¹ who postulated that 5-hydroxyisouric acid (**5**) is the primary enzymatic oxidation product. This hypothesis was well supported by electrochemical studies which showed that 5-hydroxyisouric acid formed upon nonenzymatic oxidation of urate.¹² However, the NMR data¹¹ used to support the assignment of 5-hydroxyisouric acid as the product of the urate oxidase reaction were not sufficient to rule out other structures (e.g., **3** and **4**). Therefore, we undertook a more complete characterization of the reaction product by using a full complement of specifically ¹³C-labeled urates augmented by isotope-labeling studies conducted in H₂¹⁸O. With the aid of the specifically-labeled urates, we were also able to delineate the pathway for the conversion of the enzymatic reaction product into allantoin.

In order to facilitate interpretation of the carbon chemical shifts in our system, a preliminary investigation of the ¹³C NMR properties of uric acid, allantoin, and the corresponding anions was required. Experimental measurements were correlated with properties calculated by *ab initio* methods to examine the structure of the predominant tautomeric forms of urate in neutral aqueous solution and to confirm the assignment of the product of the urate oxidase reaction.

Experimental Section

Synthesis of [¹³C]Urates. Urates, labeled specifically in one or two positions, were synthesized on a 10 mmol scale from [¹³C]urea (99 atom % ¹³C), [1-¹³C]bromoacetic acid (>99 atom % ¹³C), [2-¹³C]bromoacetic acid (99.4 atom % ¹³C) and ¹³C KCN (>99 atom % ¹³C), which were purchased from Isotec. The synthesis of uric acid was

[⊗] Abstract published in *Advance ACS Abstracts*, June 1, 1997.

(1) Mahler, H. R.; Hübscher, G.; Baum, H. *J. Biol. Chem.* **1955**, *216*, 625–641.

(2) Truscoe, R.; Williams, V. *Biochem. Biophys. Acta* **1965**, *105*, 292–300.

(3) Bongaerts, G. P. A.; Uitzetter, J.; Brouns, R.; Vogels, G. D. *Biochim. Biophys. Acta* **1978**, *527*, 348–358.

(4) Conley, T. G.; Priest, D. G. *Biochem. J.* **1980**, *187*, 727–732.

(5) Kahn, K.; Tipton, P. A. *Biochemistry* **1997**, *36*, 4731–4738.

(6) Bentley, R.; Neuberger, A. *Biochem. J.* **1952**, *52*, 694–699.

(7) For a review of the older literature, see: Vogel, G. D.; van der Drift, C. *Bacteriol. Rev.* **1976**, *40*, 403–468.

(8) Canellakis, E. S.; Cohen, P. P. *J. Biol. Chem.* **1955**, *213*, 385–395.

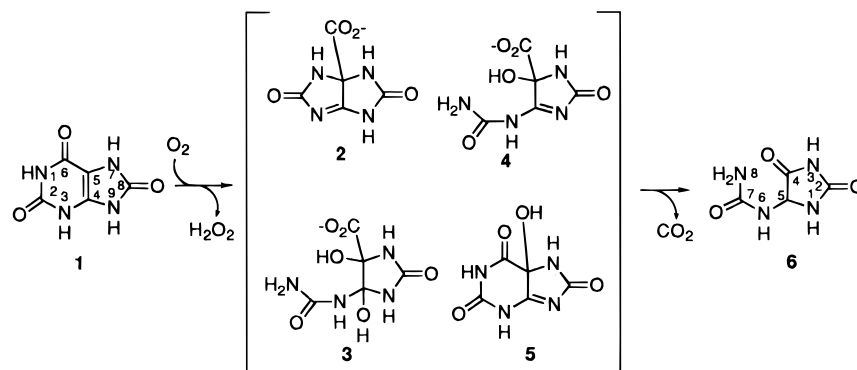
(9) Brown, G. B.; Roll, P. M.; Cavalieri, L. F. *J. Biol. Chem.* **1947**, *171*, 835.

(10) Bongaert, G. P. A.; Vogels, G. D. *Biochim. Biophys. Acta* **1979**, *567*, 295–308.

(11) Modric, N.; Derome, A. E.; Ashcroft, S. J. H.; Poje, M. *Tetrahedron Lett.* **1992**, *33*, 6691–6694.

(12) Goyal, R. N.; Brajter-Toth, A.; Dryhurst, G. *J. Electroanal. Chem.* **1982**, *131*, 181–202.

Scheme 1



accomplished using literature procedures as follows. Bromoacetic acid was converted to methyl cyanoacetate¹³ and condensed with urea⁶ to form aminouracil, which was isolated from the chilled reaction mixture by filtration. The aminouracil was converted to 5,6-diaminouracil by nitrosation and reduction;¹⁴ the crude product was recovered by filtration and was washed with H₂O and acetone. The crude bisulfite salt was suspended in concentrated HCl and warmed to 80 °C under nitrogen, which resulted in the precipitation of the HCl salt from the suspension. The diaminouracil hydrochloride was recovered by filtration and washed with H₂O and acetone. This material was immediately used for the next step in the synthesis, the condensation with urea, following the published procedure.⁶ The crude uric acid was suspended in H₂O and slowly dissolved by the gradual addition of 1 N NaOH. The pH of the solution was not allowed to exceed 9.5, since urate is susceptible to decomposition at high pH. After all of the material was dissolved, the uric acid was precipitated from solution by the addition of HCl. The product was further purified by repeated precipitations from an alkaline solution or by precipitation from a solution of concentrated sulfuric acid. The crystalline product was slightly yellow, with UV-vis and ¹³C NMR spectra matching the spectra of authentic uric acid.¹⁵ Typical yields for the overall synthesis of uric acid from bromoacetic acid and KCN were 30%. Incorporation of ¹³C into C2 of urate was accomplished by condensing [¹³C]urea with methyl cyanoacetate; [4-¹³C]urate was synthesized using K¹³CN; [5-¹³C]urate was synthesized using [2-¹³C]bromoacetic acid; [6-¹³C]urate was synthesized using [1-¹³C]bromoacetic acid; and [8-¹³C]urate was synthesized by condensing diaminouracil with [¹³C]urea.

NMR Experiments. Unlabeled allantoin (Sigma Chemical Co.) and specifically ¹³C-labeled uric acids in 100 mM phosphate (D₂O) were used to study the pH dependence of the carbon chemical shifts. To generate and study the product of the urate oxidase reaction, 5 mM solutions of [¹³C]urate were prepared in 100 mM phosphate, pH 7.6 in 100% D₂O. The solution was degassed and then saturated with oxygen in a small round-bottom flask using a Firestone valve. In a typical experiment, 0.7 units of purified soybean root nodule urate oxidase, either native enzyme⁵ or recombinant enzyme expressed in *Escherichia coli* as a thioredoxin fusion protein,¹⁶ was added to the oxygenated urate solution. After 5 min, catalase (400 units) was added to remove hydrogen peroxide. Control experiments showed that the same oxidation products formed in the absence as in the presence of catalase. The reaction mixture was gently bubbled with oxygen for 15 min, and the progress of the reaction was monitored spectrophotometrically (urate has an absorption maximum at 292 nm while the product has increased absorbance relative to urate between 302 and 306 nm). The solution was then transferred to a 5 mm NMR tube and spectra were acquired

for several hours. The ¹³C NMR spectra were proton decoupled and were collected with a sweep width of 49682 Hz at 17 °C with a Bruker AVANCE DRX500 instrument; 128 scans were sufficient to detect the signal due to the primary oxidation product. Higher spectral resolution (0.2 Hz versus 0.6 Hz), lower temperature (5 °C), and longer acquisition times (1024 scans) were used in experiments conducted with H₂¹⁸O (>99 atom % ¹⁸O, purchased from Isotec). The spectra in H₂¹⁸O were resolution enhanced with a Gaussian window function. 1,4-Dioxane (66.5 ppm) served as an internal chemical shift standard.

Computational Methods. An *ab initio* quantum mechanical approach was used to study uric acid, urate mono- and dianions, and the oxidation products. All calculations were performed with Gaussian 92^{17a} and Gaussian 94^{17b} programs. Uric acid, the four possible urate monoanions, and the six possible urate dianions were optimized at the HF/6-31+G(d,p) level, and frequency analysis was performed to verify the minima. The structures were kept planar, and energy was minimized with respect to all geometrical parameters unless frequency analysis indicated that the planar structure was not the minimum energy structure. In the latter cases, the nonplanar structures were optimized without constraints. The stability of the restricted Hartree-Fock (RHF) wave function was tested for uric acid and for the urate monoanions; the wave functions showed real stability. A value of 0.92 was used as a correction factor to scale the HF/6-31+G(d,p) zero-point energies.¹⁸ Urate monoanions were also optimized at the MP2(Full)/6-31+G(d) level and in the presence of a solvent reaction field at the HF/6-31+G(d) level using the Onsager self-consistent reaction field model.¹⁹ Two tautomers of 5-hydroxyisouric acid and their corresponding monoanions were optimized at the HF/6-31+G(d,p) level.

Calculations of NMR spectra were performed by the GIAO method²⁰ in Gaussian 94 using a density functional theory approach. The most satisfactory results were obtained using Becke's exchange functional²¹ with the Lee, Yang, and Parr (LYP) correlation functional.²² Two basis sets, D95+(2d,p) and AUG-cc-pVDZ, were chosen for NMR calculations on the basis of the results of preliminary calculations of acetone and uric acid shieldings. The geometries used for NMR calculations were optimized at the B3LYP/6-31++G(2d,p) level. Calculated shieldings were converted to chemical shift values by the formula $\delta =$

(13) Lazarus, R. A.; Sulewski, M. A.; Benkovic, S. J. *J. Labelled Compd. Radiopharm.* **1982**, *19*, 1189–1195.

(14) Sherman, W. R.; Taylor, E. C. *Organic Syntheses*; Wiley: New York, 1963; Collect. Vol. 4, pp 247–249.

(15) Coxon, B.; Fatiadi, A. J.; Sniegoski, L. T.; Hertz, H. S.; Schaffer, R. *J. Org. Chem.* **1977**, *42*, 3132–3140.

(16) The urate oxidase-thioredoxin fusion protein was created by splicing the gene encoding soybean root nodule urate oxidase⁵ in-frame to the pThioHis A vector (Invitrogen). This protein was expressed and purified in the same manner as the recombinant protein;⁵ no significant differences in kinetic behavior were noted between the fusion protein, the recombinant protein, and native enzyme isolated from soybean root nodules.

(17) (a) Frisch, M. J.; Trucks, G. W.; Head-Gordon, M.; Gill, P. M. W.; Wong, M. W.; Foresman, J. B.; Johnson, B. G.; Schlegel, H. B.; Robb, M. A.; Replogle, E. S.; Gomperts, R.; Andres, J. L.; Raghavachari, K.; Binkley, J. S.; Gonzalez, C.; Martin, R. L.; Fox, D. J.; Defrees, D. J.; Baker, J.; Stewart, J. P.; Pople, J. A. *Gaussian 92*; Gaussian, Inc.: Pittsburgh, PA, 1992. (b) Frisch, M. J.; Trucks, G. W.; Schlegel, H. B.; Gill, P. M. W.; Johnson, B. G.; Robb, M. A.; Cheeseman, J. R.; Keith, T.; Petersson, G. A.; Montgomery, J. A.; Raghavachari, K.; Al-Laham, M. A.; Zakrzewski, V. G.; Ortiz, J. V.; Foresman, F. B.; Cioslowski, J.; Stefanov, B. B.; Nanayakkara, F.; Challacombe, M.; Peng, C. Y.; Ayala, P. Y.; Chen, W.; Wong, M. W.; Andres, J. L.; Replogle, E. S.; Gomperts, R.; Martin, R. F.; Fox, D. J.; Binkley, J. S.; Defrees, D. J.; Baker, J.; Stewart, J. P.; Head-Gordon, M.; Gonzalez, C.; Pople, J. A. *Gaussian 94*, Rev. C.3; Gaussian, Inc.: Pittsburgh, PA, 1995.

(18) Scott, A. P.; Radom, L. *J. Phys. Chem.* **1996**, *100*, 16502–16513.

(19) Wong, M. W.; Frisch, M. J.; Wiberg, K. B. *J. Am. Chem. Soc.* **1991**, *113*, 4776–4782.

(20) Wolinski, K.; Hilton, J. F.; Pulay, P. *J. Am. Chem. Soc.* **1990**, *112*, 8251–8260.

(21) Becke, A. D. *Phys. Rev. A* **1988**, *38*, 3098–3100.

(22) Lee, C.; Yang, W.; Parr, R. G. *Phys. Rev. B* **1988**, *37*, 785–789.

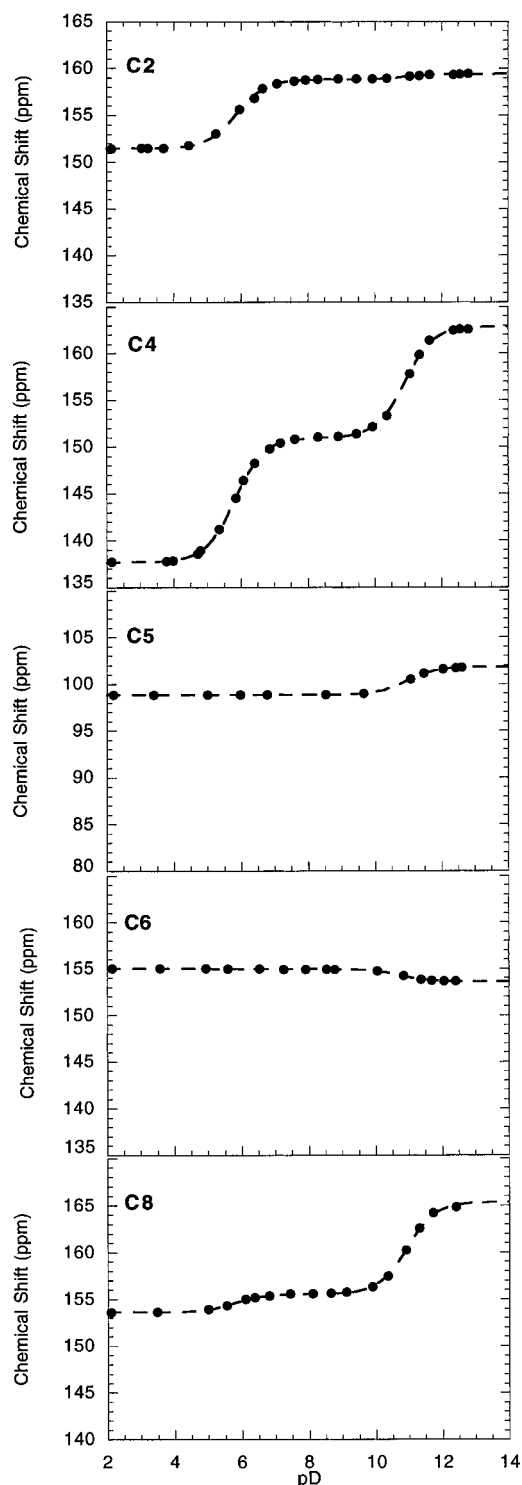


Figure 1. ^{13}C NMR titration of uric acid **1** in 0.1 M phosphate in D_2O . Dioxane was used as an internal chemical shift standard (66.5 ppm).

$\sigma_{\text{Acetone}} - \sigma_{\text{X}} + 201.2$ where σ_{Acetone} is the calculated shielding of the carbonyl of acetone at the appropriate level of theory, σ_{X} is the shielding of the carbon under study and 201.2 is the experimental gas phase chemical shift of the acetone carbonyl relative to tetramethylsilane.²³ The geometries of the structures that were used for NMR calculations, and the calculated shielding values with the D95+(2d,p) and AUG-cc-pVDZ basis sets are included in the Supporting Information.

Results

Ionization Equilibria of Uric Acid and Allantoin. The results of the titration of the labeled uric acids in D_2O are shown

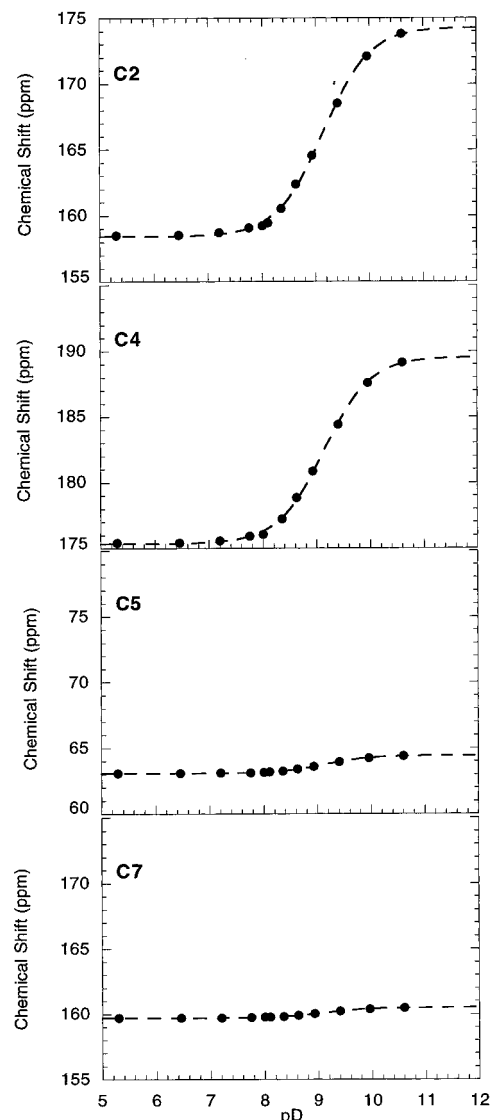


Figure 2. ^{13}C NMR titration of allantoin (**6**) in 0.1 M phosphate in D_2O . Dioxane was used as an internal chemical shift standard (66.5 ppm).

in Figure 1. These titration curves defined pK_a values of 5.80 ± 0.07 and 10.85 ± 0.1 . It is apparent from the magnitudes of the changes in the chemical shifts at C2 and C4 that the site of the first ionization is N3. The dianion appears to be the N3,N9-deprotonated species. The titration curves of allantoin are shown in Figure 2. The pK_a of allantoin was determined to be 9.14 ± 0.03 in D_2O , and the site of ionization of allantoin appears to be N3, based on the magnitude of the changes in the chemical shifts of C2 and C4. The pK values determined by these experiments are in good agreement with previously determined values (*vide infra*). The knowledge of the precise chemical shifts of urate and allantoin as a function of pH was invaluable for identifying species in complex reaction mixtures. It is important to note that at some pH values the chemical shifts for some carbons coincide (e.g., C2 and C8 of urate and C2 and C7 of allantoin); this can be a source of confusion if not recognized.

Identification of the Urate Oxidase Reaction Products.

Each of the five individually ^{13}C -labeled urates were utilized as substrates for urate oxidase, and the ^{13}C NMR signals of the resulting products were recorded. The time courses of the

(23) Jameson, A. K.; Jameson, C. J. *Chem. Phys. Lett.* **1987**, *134*, 461–466.

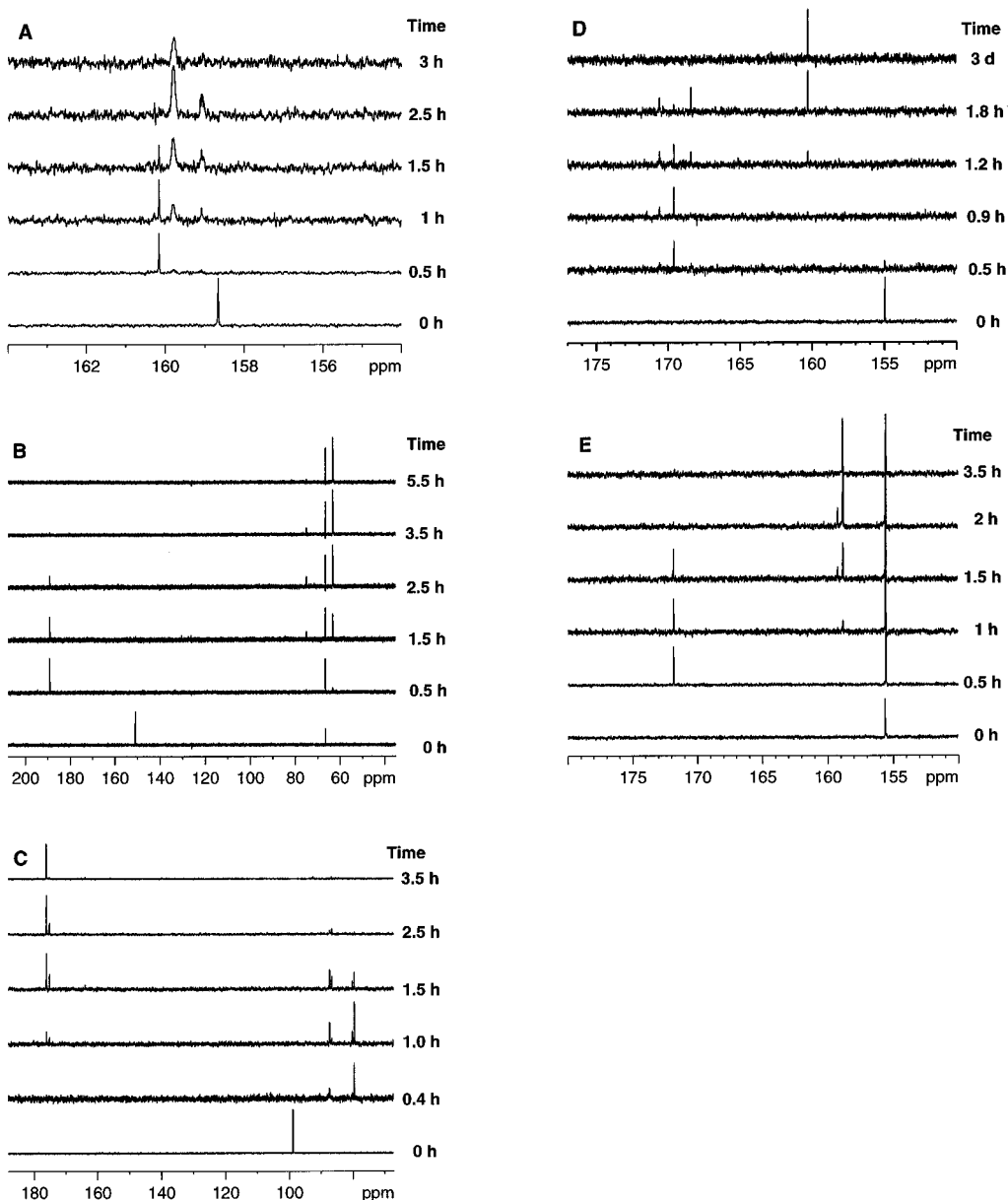


Figure 3. Time courses of the urate oxidase-catalyzed oxidation of [^{13}C]urate: (A) [$2\text{-}^{13}\text{C}$]urate; (B) [$4\text{-}^{13}\text{C}$]urate; (C) [$5\text{-}^{13}\text{C}$]urate; (D) [$6\text{-}^{13}\text{C}$]urate; (E) [$8\text{-}^{13}\text{C}$]urate. Spectra were collected at 17 °C in 0.1 M sodium phosphate in 70% D_2O .

reaction (Figure 3) show rapid formation of the primary oxidation product and the subsequent decay of that species into allantoin. The primary product was optically active, based on circular dichroism spectropolarimetric measurements (data not shown). The decay of this species followed first order kinetics; at 17 °C it had a half-life of 30 min. At least two species intervene between the primary oxidation product and allantoin; this is most clearly visible in the time course obtained with [$6\text{-}^{13}\text{C}$]urate. The structures of the reaction products were further probed by conducting reactions in 50% H_2^{18}O . The ^{18}O -induced shift in the C5 signal of the primary reaction product (Figure 4) indicates that a water-derived oxygen is connected to this carbon. In a similar experiment conducted with [$6\text{-}^{13}\text{C}$]urate, the primary reaction product showed no isotope shift, confirming that the peak at 169.6 ppm is due to a carbonyl carbon, not a carboxylate carbon. However, the species which formed from the primary oxidation product generated from [$6\text{-}^{13}\text{C}$]urate did show an ^{18}O isotope shift in the peak at 170.6 ppm (data not shown) indicating that it arises from the hydrolysis of the primary reaction product. By using [$4,6\text{-}^{13}\text{C}_2$] uric acid, we observed that the species formed by hydrolysis is also

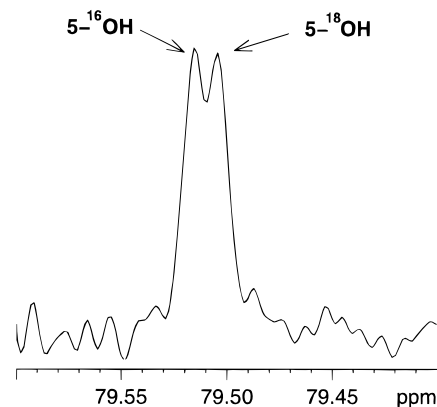


Figure 4. ^{13}C NMR spectrum of the primary oxidation product, identified as **8**, from [$5\text{-}^{13}\text{C}$]urate, in 50% H_2^{18}O .

unstable and rearranges into a structure where C6 of urate is directly bonded to C4 of urate. Figure 5 shows the appearance of strong carbon–carbon coupling ($J_{\text{CC}} = 53$ Hz) in this species. Allantoin was the only stable product formed in aqueous

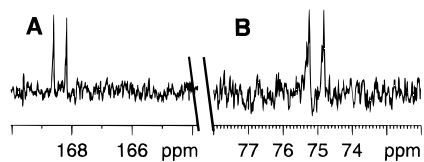


Figure 5. ^{13}C NMR spectrum of the third transiently-formed species, identified as **12**, from $[4,6-^{13}\text{C}_2]\text{urate}$: (A) signal from C6 (urate numbering scheme); (B) signal from C4.

Table 1. Calculated Gas-Phase SCF Energies (au), Zero-Point Energies (kcal/mol) and Entropies (cal/mol K) at the HF/6-31+G(d,p) Level for Uric Acid and Urate Anions

compound	SCF energy	ZPE	entropy
uric acid	-634.157403070	73.89	93.558
N3 urate anion	-633.632720283	65.14	96.304
N9 urate anion	-633.629442932	65.59	90.958
N1 urate anion	-633.596841430	64.48	95.108
N7 urate anion	-633.594766286	64.64	92.944
N3,N9 dianion	-632.939308258	56.68	89.310
N1,N9 dianion	-632.930609284	56.34	91.063
N3,N7 dianion	-632.930579809	56.50	89.625
N1,N3 dianion	-632.901967766	55.96	92.841
N1,N7 dianion	-632.899412867	55.79	91.486
N7,N9 dianion	-632.899056297	56.25	90.694

solutions at pH 7–8 when phosphate or tris buffer was used. It should be noted that allantoin derived from $[2-^{13}\text{C}]\text{urate}$ was labeled exclusively at C7, and allantoin derived from $[8-^{13}\text{C}]\text{urate}$ was labeled only at C2 (the numbering of atoms of allantoin (**6**) and uric acid (**1**) are shown in Scheme 1). This observation implies that no symmetrical intermediate lies on the pathway between urate and allantoin. However, we noted that after its formation, scrambling of the C2 and C7 atoms of allantoin did occur over time (data not shown).

Computational Results

Structures and Energies. The *ab initio* energies of the optimized uric acid and its mono- and dianions at HF/6-31+G(d,p) level are shown in Table 1. The planar form was the minimum energy conformation for uric acid as indicated by the frequency analysis at the HF/6-31+G(d,p) and B3LYP/6-31++G(2d,p) levels. Urate mono- and dianions were planar or very close to planar with some nitrogen centers being slightly pyramidal. The MP2 and B3LYP structures of uric acid were very similar to each other and had ca. 0.015 Å longer bond lengths than the corresponding HF structure; the increase of the basis set from 6-31G(d) to 6-31++G(2d,p) resulted in a small contraction of bond lengths. The overall B3LYP/6-31++G(2d,p) structure had a root mean square (rms) error of 0.02 Å when the heavy atom distances from the gas-phase calculations were compared to an available X-ray structure of uric acid.²⁴ The MP2(Full)/6-31+G(d) energies for urate monoanions are as follows (in kcal/mol): N3 anion -635.495049855; N9 anion -635.494070047; N7 anion -635.467489640; N1 anion -635.464484854. The Onsager SCRF solvation energies at the HF/6-31+G(d) level are as follows (in kcal/mol): N3 anion 1.05; N9 anion 2.40; N7 anion 8.46; N1 anion 9.75. 5-Hydroxy- $\Delta^{3,4}$ -isouric acid was more stable than 5-hydroxy- $\Delta^{4,9}$ -isouric acid by 0.84 kcal/mol at the HF/6-31+G(d,p) level. At the HF 6-31+G(d,p) and B3LYP 6-31++G(2d,p) levels, N9-deprotonated 5-hydroxy- $\Delta^{3,4}$ -isourate was the most stable tautomer of 5-hydroxyisourate, followed by N1-deprotonated 5-hydroxy- $\Delta^{4,9}$ -isourate.

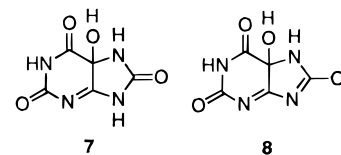
GIAO NMR Spectra. ^{13}C NMR spectra were calculated in order to confirm the assignment of the structure of the metastable

Table 2. Calculated ^{13}C NMR Chemical Shifts (ppm)

compound	exptl (D ₂ O)	D95+(2d,p)	AUG-cc-pVDZ
Uric Acid (1)			
C2	151.5	144.8	144.3
C4	137.8	130.5	129.5
C5	98.8	100.3	99.0
C6	155.0	148.9	147.3
C8	153.6	144.5	144.6
Urate (9)			
C2	158.8	156.7	155.4
C4	150.6	148.3	146.7
C5	98.8	97.6	95.5
C6	155.0	152.4	150.4
C8	155.6	147.7	147.7
5-Hydroxyisourate (8)			
C2	160.2	154.2	152.8
C4	189.0	184.4	182.9
C5	79.4	82.5	83.1
C6	169.6	170.0	169.5
C8	171.8	171.6	170.6

product of the urate oxidase reaction. Preliminary work indicated that NMR calculations based on HF wave functions were not of sufficient accuracy for this purpose and suffered from being strongly basis set dependent. The importance of electron correlation in NMR calculations, particularly in compounds with multiple bonds, has been illustrated recently.²⁵ Since MBPT(2) calculations on hydroxyisourate would have been prohibitively costly, the more economical DFT approach was explored and found to be satisfactory. The results of these calculations are summarized in Table 2. Our best results were obtained with the D95+(2d,p) and AUG-cc-pVDZ basis sets and were able to reproduce the ^{13}C NMR spectrum of uric acid with a rms error of 6 ppm. The calculated gas phase chemical shifts were slightly upfield relative to experimental chemical shifts measured in aqueous solution; this difference may arise from the deshielding effect of the medium²³ or reflect the inaccuracy of *ab initio* NMR calculations. However, the calculated ^{13}C NMR spectrum of the N3-deprotonated urate monoanion reproduced the experimental spectrum more closely, with a rms of 4 ppm. This increased accuracy may be the result of the decreased conjugation in the monoanion.

In order to assign the structure for the observed product of the urate oxidase reaction, the NMR spectra of 5-hydroxy- $\Delta^{4,9}$ -isouric acid (**5**), 5-hydroxy- $\Delta^{3,4}$ -isouric acid (**7**), and N9-deprotonated 5-hydroxy- $\Delta^{3,4}$ -isourate (**8**) were calculated. The



rms error between calculated and observed ^{13}C shifts were 3.7 ppm for **8**, 11.2 ppm for **5**, and 14.3 ppm for **7**. The NMR spectrum of N1-deprotonated 5-hydroxy- $\Delta^{4,9}$ -isourate was also calculated; the ^{13}C shifts had an rms error of 6.4 ppm. The shielding values for each carbon in these compounds are given in the Supporting Information, and the chemical shifts for the carbons in **8** are listed in Table 2.

Discussion

Ionization of Uric Acid. The structure of the predominant urate monoanion has been a subject of disagreement in the

(24) Ringertz, H. *Acta Crystallogr.* **1966**, *20*, 397–403.

(25) Gauss, J. *J. Chem. Phys.* **1993**, *99*, 3629–3643.

literature. Both N3-deprotonated²⁶ and N9-deprotonated²⁷ forms have been suggested to prevail in aqueous solutions. In the crystals of Na and Mg salts of urate, N3 is deprotonated.²⁸ The pK_a value for the first acid dissociation constant has been found to be 5.27 by spectrophotometric titration^{26a} and 5.53 by potentiometric titration.^{26b} Values of 9.8,^{27b} 10.5,^{26b} and 10.9^{26a} have been reported for the second acid dissociation constant. Figure 1 illustrates the results of the titration of the specifically ¹³C-labeled uric acids in D₂O with NaOD. The first ionization is accompanied by a large downfield shift at C2 and C4, while upon the second ionization C4 and C8 carbons undergo a significant downfield shift. There is a small downfield shift in C8 signal during the first ionization, but no shift in the C2 signal occurs as the second proton dissociates. These changes in chemical shifts represent the true ionic equilibrium between species and are not due to decomposition of urate at high pH, as demonstrated by the fact that identical results were obtained by titrating alkaline urate solutions with phosphoric acid. We conclude from these data that the N3-deprotonated tautomer predominates strongly over the N9-deprotonated tautomer in aqueous solutions. The pK values determined here, 5.80 ± 0.07 and 10.85 ± 0.1 , were measured in D₂O and are higher than the corresponding values in H₂O due to the solvent isotope effect. The magnitude of the solvent isotope effect for organic acids is typically 0.5 pH units.²⁹ The correction for the solvent isotope effect gives values of 5.3 and 10.3 for the pK values of urate, which are consistent with literature values.

The relative stabilities of the urate mono- and dianions were predicted with *ab initio* methods using HF and MP2 theories. Data in Table 1 show that the N3-deprotonated monoanion is more stable than the N9-deprotonated monoanion at the HF/6-31+G(d,p) level by 2.5 kcal/mol after correction for differences in zero-point energies. The N1-deprotonated and N7-deprotonated anions are higher in energy than the N3-deprotonated anion by 21.9 and 23.4 kcal/mol, respectively. To extrapolate these gas-phase results into free energy differences in aqueous solution at room temperature, the contributions from thermal energies, entropy, and solvation energy must be included. Clearly, the solvation energy contribution is the most difficult to determine due to multiple possible hydrogen-bonding interactions between solute and solvent. Although the absolute magnitude of solvation energies is uncertain for the urate monoanion, one may reasonably expect that solvation contributions due to hydrogen bonding with water will be very similar for the four monoanions. The differences in dipolar contributions can still be important and these were estimated using the Onsager SCRF model. The estimated free energies at the HF level in condensed media with a value for ϵ of 78.0, relative to the N3-deprotonated monoanion, are N9 anion +2.7 kcal/mol, N1 anion +13.5 kcal/mol, and N7 anion +16.9 kcal/mol. We also tested the effect of electron correlation on the relative energies of urate tautomers, since electron correlation has been shown to be important in other heterocyclic equilibria.³⁰ The MP2/6-31+G(d) energies were corrected for zero-point energy, thermal, entropic, and solvation contributions; the order of

Table 3. Observed ¹³C NMR Chemical Shifts for Urate, the Urate Oxidase Reaction Product, and Subsequent Decay Products^a

	9	8	4	12	13
C2 ^b	158.8	160.2	nd ^c	159.1	159.8
C4	151.0	189.0	nd	75.0	63.2
C5	98.9	79.4	87.2	175.1	175.7
C6	155.0	169.6	170.6	168.3	(160.3 ^d)
C8	155.6	172.0	164.5	159.2	159.0

^a Chemical shifts are in ppm, relative to TMS. ^b Atom numbering schemes are based on the urate carbon skeleton. ^c nd, not detected; no signal could be detected for these species. ^d HCO₃⁻.

stabilities (in kcal/mol) was N3 anion 0.0, N9 anion +1.3, N1 anion 10.2, and N7 anion 10.6. The MP2 free energy difference corresponds to a pK difference of 0.95 pH units between the N3 and N9 monoanions, in good agreement with the experimentally measured pK difference of 1.1 pH units for 3-methyl and 9-methyl analogs of uric acid.^{26b} MP2 results imply that the N3-deprotonated anion predominates over the N9-deprotonated anion by a factor of 9 in solution. This conclusion is further supported by good agreement between the observed ¹³C NMR spectrum of urate in aqueous solution and the calculated spectrum of the N3-deprotonated urate. The *ab initio* energies for dianions indicate that the N3,N9-deprotonated dianion is 4.6 kcal/mol more stable than the next most stable species, the N1,N9-deprotonated tautomer in the gas phase. Thus, both experimental determinations and theoretical predictions suggest that the N3-deprotonated urate monoanion is the predominant species in neutral aqueous solutions, while in strongly alkaline environment the N3,N9-deprotonated dianion prevails.

Ionization of Allantoin. A value of 8.6 for the acid dissociation constant of allantoin at 30 °C has been determined previously,³¹ but the tautomeric structure of the anion was not identified. Our NMR titration results shown in Figure 2 indicate that allantoin ionizes at N3; the observed pK_a of 9.14 in D₂O is in excellent agreement with the literature value after correction for the solvent isotope effect. The structure of the anion is of interest since the anion racemizes about 5000 times more rapidly than the neutral form³¹ and racemization, if it occurs via formation of a bicyclic intermediate, could lead to scrambling of the atoms of the hydantoin and urea moieties of allantoin. Indeed, such scrambling has been observed in the enzymatic oxidation of ¹⁵N-enriched urate⁹ and [8-¹⁴C]urate;⁸ these results were used to support the notion that a symmetrical intermediate forms on the pathway from urate to allantoin.

Identification of the Product of the Urate Oxidase Reaction. It is evident from the data shown in Figure 3 that urate oxidase converts urate to a metastable species which decays nonenzymatically to form allantoin. The ¹³C NMR chemical shifts of this species are summarized in Table 3. As shown in Figure 4, an oxygen from solvent water is incorporated into the primary reaction product at C5, presumably in the form of a hydroxyl group. On the basis of this observation and chemical shift considerations, the true product of the urate oxidase reaction is proposed to be 5-hydroxyisourate. The downfield shifts of C4 and C8 are consistent with the tautomeric structure of **8**. In order to confirm this assignment, the ¹³C NMR spectrum of **8** was calculated using density functional theory; as shown in Table 2, the agreement between the calculated spectrum and that observed experimentally is quite good. The calculations also revealed that **8** is the most stable tautomer of 5-hydroxyisourate. Compounds **2**,³² **3**, and **4**¹⁰ have also been suggested as candidates for the product of the enzymatic reaction.

(26) (a) Pfeleiderer, W. *Liebigs Ann. Chem.* **1974**, 2030–2045. (b) Smith, R. C.; Gore, J. Z.; McKee, M.; Hargis, H. *Microchem. J.* **1988**, 38, 118–124.

(27) (a) Bergmann, F.; Dikstein, S. *J. Am. Chem. Soc.* **1955**, 77, 691–696. (b) Simic, M. G.; Jovanovic, S. L. *J. Am. Chem. Soc.* **1989**, 111, 5778–5782.

(28) (a) Mandel, N. S.; Mandel, G. J. *J. Am. Chem. Soc.* **1975**, 98, 2319–2323. (b) Dubler, E.; Jameson, G. B.; Kopajtic, Z. *J. Inorg. Biochem.* **1986**, 26, 1–21.

(29) Schowen, K. B.; Schowen, R. L. *Methods Enzymol.* **1982**, 87, 551–606.

(30) Cramer, C. J.; Truhlar, D. G. *J. Am. Chem. Soc.* **1993**, 115, 8810–8817.

(31) Vogels, G. D.; De Windt, F. E.; Bassie, W. *Recl. Trav. Chim.* **1969**, 88, 940–950.

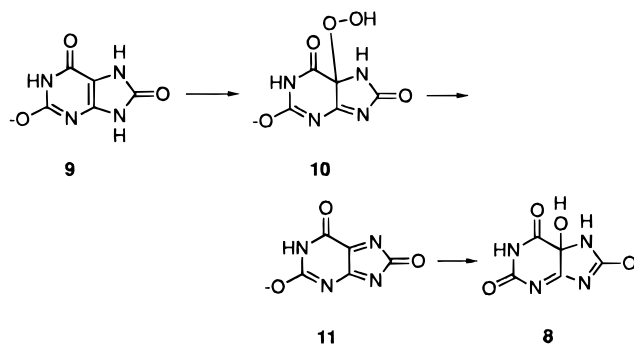
(32) Conley, T. G.; Priest, D. G. *Biochem. J.* **1980**, 187, 733–738.

However, **2** can be excluded on the basis of our observation that ^{18}O is incorporated from solvent into the reaction product at C5. Compounds **3** and **4** can be excluded from consideration on the basis of the observation that the primary reaction product does not show incorporation of ^{18}O from solvent into C6. 5-Hydroxyisourate has previously been proposed to be the product of the urate oxidase reaction;¹¹ however, that assignment was based on a single ^{13}C chemical shift value obtained using [$5\text{-}^{13}\text{C}$]urate as substrate. Furthermore, the signal reported in that work appeared at 87.5 ppm and does not correspond with the C5 signal at 79.4 ppm which we have observed. We found that the primary oxidation product underwent hydrolysis, and the ^{13}C signal for C5 in the hydrolysis product **4** appeared at 87.2 ppm; therefore it is possible that in the previous work **4** was observed, rather than 5-hydroxyisourate.

The product of the pterin-utilizing enzyme phenylalanine hydroxylase has also been identified on the basis of ^{13}C NMR studies, and the structural similarities between pterin and urate are striking. In the phenylalanine hydroxylase reaction, C4a of the substrate 6-methyltetrahydropterin has a chemical shift of 98.9 ppm, and it was converted to a species in which the ^{13}C NMR signal for C4a shifted upfield to 72.3 ppm. On the basis of this observation and the fact that an oxygen atom derived from molecular oxygen was incorporated into the product at C4a, 4a(*S*)-hydroxy-6-methyltetrahydropterin was proposed to be the product of the phenylalanine hydroxylase reaction.³³ The chemical shift changes observed in the phenylalanine hydroxylase reaction are quite similar to those observed in the urate oxidase reaction, as are the structures of the proposed products, although the origin of the oxygen incorporated into the products is different.

The structural similarities between urate, pterin, and reduced flavin suggest a possible mechanism for the urate oxidase reaction. One of the confounding features of urate oxidase has been the absence of evidence for a cofactor.⁵ However, it is possible that oxygen and urate can react directly in a manner reminiscent of flavin and pterin reactions with oxygen. It is generally believed that the reactions between flavin or pterin and molecular oxygen occur via single-electron transfers in order to relieve the restriction on direct reactions between singlet and triplet species,³⁴ and it is their ability to form relatively stable radicals which is invoked to explain their participation in biological redox reactions.³⁵ The radical formed from one-electron oxidation of urate has been observed under physiological conditions as well,³⁶ and the one-electron redox potential of the urate dianion is 0.26 V.³⁷ Steady-state kinetic studies suggest that the urate monoanion binds to urate oxidase and that the enzyme active site contains a residue which abstracts a proton from urate during the course of the catalytic reaction.⁵ A possible chemical mechanism for the urate oxidase reaction based on these considerations is shown in Scheme 2. The exact nature of the oxidation step has been left ambiguous; we cannot distinguish between a mechanism in which a discrete C5 urate hydroperoxide is formed as an intermediate, and a mechanism in which direct electron transfer from urate to molecular oxygen occurs. The species **11** which is proposed would form directly as a result of electron transfer or via collapse of the urate hydroperoxide; **11** has been proposed to be the product of the

Scheme 2



electrochemical oxidation of urate and was observed to add water in a rapid first-order reaction.³⁸ We propose that, in the enzymatic reaction, the hydration of **11** occurs at the active site, because the observed product **8** is optically active.

Mechanism of Allantoin Formation. Although 5-hydroxyisourate is the immediate product of the urate oxidase reaction, it is evident from Figure 3 that allantoin and CO_2 are the ultimate products. The NMR time courses demonstrate that the formation of allantoin occurs via at least two observable intermediates. At least three different models for the decomposition of 5-hydroxyisouric acid have been suggested in the recent literature: (a) hydration across the N3–C4 bond followed by hydrolysis of the C5–C6 bond to form a keteneimine,³⁹ (b) hydrolysis of the N1–C6 bond,¹¹ and (c) contraction of the 6-membered ring to form **2**.⁴⁰ When the reaction was conducted in H_2^{18}O , we observed that the signal from C6 showed an isotope shift in the species arising from 5-hydroxyisourate, indicating that the decomposition was hydrolytic and ruling out the formation of a keteneimine species. The observation that the ^{13}C labels at C2 and C8 of urate do not become scrambled in allantoin demonstrates that no symmetrical species is formed on the pathway to allantoin, ruling out the formation of **2**. The positions of the NMR signals as well as the ^{18}O labeling data are most consistent with the structure **4** (and with its hydrated form **3**), indicating that 5-hydroxyisourate decomposes by hydrolysis of the N1–C6 bond. Both **3** and **4** have been suggested to be part of the allantoin formation pathway. We were not able to detect an NMR signal corresponding to **4** when it was produced from [$4\text{-}^{13}\text{C}$]urate, even under conditions in which signals from the other carbons were well defined. This could be due to the long relaxation time of this carbon, but the more likely cause is the attenuation of the signal due to exchange broadening. Exchange broadening can be also observed by closer inspection of the resonance of the C5 signal at 87.3 ppm. Therefore, the available data suggest that an equilibrium between **3** and **4** is established.

It is apparent from the time courses that another species lies on the pathway from **4** to allantoin. Surprisingly, the experiment conducted with [$6\text{-}^{13}\text{C}$]urate showed that the carboxylate group was still present in this intermediate, giving rise to a signal at 168.3 ppm. A carbon skeleton rearrangement has been documented in the alkaline oxidation of uric acid to form uroanate, and on the basis of these data, it was proposed that **4** undergoes a 1,2-carboxylate shift in the conversion to allantoin.⁴¹ In order to test this proposal directly, we prepared [$4,6\text{-}^{13}\text{C}_2$]urate and monitored its conversion to allantoin. As shown in Figure 5, in the species which forms from **4**, the signals from C4 and C6

(33) Lazarus, R. A.; deBrosse, C. W.; Benkovic, S. J. *J. Am. Chem. Soc.* **1982**, *104*, 6869–6871.

(34) Massey, V. *J. Biol. Chem.* **1994**, *269*, 22459–22462.

(35) Walsh, C. *Enzymatic Reaction Mechanisms*; W. H. Freeman and Company: San Francisco, CA, 1979; pp 358–431.

(36) Maples, K. R.; Mason, R. P. *J. Biol. Chem.* **1988**, *263*, 1709–1712.

(37) Jovanovic, S. V.; Simic, M. G. *J. Phys. Chem.* **1986**, *90*, 974–978.

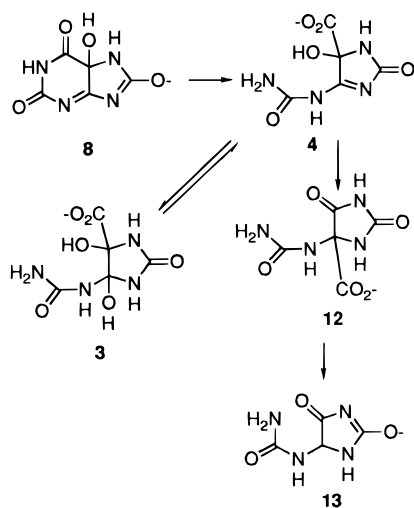
(38) Wrona, M. A.; Owens, J. L.; Dryhurst, G. *J. Electroanal. Chem.* **1979**, *105*, 295–315.

(39) Brajter-Toth, A.; Dryhurst, G. *J. Electroanal. Chem.* **1981**, *122*, 205–213.

(40) Goyal, R. N.; Brajter-Toth, A.; Dryhurst, G. *J. Electroanal. Chem.* **1982**, *131*, 181–202.

(41) Poje, M.; Sokolic-Maravic, L. *Tetrahedron* **1988**, *44*, 6723–6728.

Scheme 3



each appear as doublets with a coupling constant of 53 Hz. The observed value of the coupling constant in this intermediate is in good agreement with the J_{CC} values observed for the carboxyl and α -carbon couplings in amino acids.⁴² Thus, these data provide direct evidence for the 1,2-carboxylate shift proposed earlier which leads to the formation of **12**.⁴¹ Decarboxylation of **12** yields allantoin; the proposed pathway for conversion of 5-hydroxyisourate to the observed tautomer of the allantoin anion **13** is shown in Scheme 3.

It is not easy to rationalize why **4** undergoes the observed 1,2-carboxylate shift to form **12**, instead of decarboxylating to yield the enol tautomer of allantoin directly. However, it is equally difficult to arrive at another interpretation of the available data. The possibility that the NMR signals shown in Figure 5 arise not from a single species exhibiting ^{13}C – ^{13}C coupling but from two species whose ^{13}C NMR signals are fortuitously spaced, can be excluded because if an additional species were present, it would have been apparent in experiments conducted with singly-labeled urate as well. The original suggestion that this rearrangement occurs was based on the observation that alkaline oxidation of [^{14}C]urate resulted in the formation of [^{14}C]uroxanate (bis(ureido)malonate);⁴¹ it is also difficult to suggest a reasonable alternative explanation for these data. However, it is important to note that neither the experiments reported here nor those described earlier⁴¹ establish that direct decarboxylation of **4** does not occur, to some extent, in competition with the carboxylate shift. Examination of Figure

3D reveals that HCO_3^- becomes detectable at the same time as **12**, within the temporal resolution of this experiment. In their work, Poje and Sokolic-Maravic, reported formation of a significant amount of [^{14}C]allantoin,⁴¹ which could have arisen from decarboxylation of **4** or **12**. Presumably, a careful kinetic analysis of the reaction could determine whether **12** is an obligatory intermediate in the conversion of **4** to allantoin; however, the experiments illustrated in Figure 3 were not conducted in such a manner that the concentration of the detectable intermediates could be determined accurately.

It is important to note that the regiochemistry of urate is preserved in its conversion to allantoin (i.e., C2 of urate becomes C7 of allantoin and C8 of urate becomes C2 of allantoin). Early reports that isotopic labels in urate became scrambled during its conversion to allantoin^{8,9} provided a major conceptual barrier to understanding the mechanism of allantoin formation. Sokolic et al. first provided evidence that scrambling does not occur during the urate oxidase reaction;⁴³ our observations are in accord with theirs. We have determined, however, that scrambling does occur at physiological pH after allantoin is formed, and the mechanisms by which this occurs are currently under investigation.

Conclusions

The N3-deprotonated urate monoanion is the predominant tautomeric form in neutral aqueous solutions of urate. Its urate oxidase mediated oxidation with molecular oxygen yields N9-deprotonated 5-hydroxyisourate and H_2O_2 . The overall oxidation of urate is likely to be similar in mechanism to the enzymatic oxidation of reduced flavin and tetrahydropterin by molecular oxygen. 5-Hydroxyisourate undergoes nonenzymatic hydrolysis at the N1–C6 bond followed by migration of the carboxylate group to C4 and subsequent decarboxylation to give allantoin and CO_2 as the final stable products.

Acknowledgment. We thank Dr. Wei Wycoff for experimental assistance; valuable discussions with Professor Rainer Glaser (University of Missouri—Columbia) about computational chemistry are most appreciated. This work was supported by grant 96-35305-3543 from the USDA NRICGP. The NMR spectrometers used in this work were supported by NSF grant 8908304.

Supporting Information Available: Energy-minimized structures and calculated shieldings of acetone, uric acid, N3-deprotonated urate, 5-hydroxy- $\Delta^{3,4}$ -isouric acid, 5-hydroxy- $\Delta^{4,9}$ -isouric acid, N9-deprotonated 5-hydroxy- $\Delta^{3,4}$ -isourate, and N1-deprotonated 5-hydroxy- $\Delta^{4,9}$ -isourate (7 pages). See any current masthead page for ordering and Internet access instructions.

(42) Wray, V.; Hansen, P. E. In *Annual Reports on NMR Spectroscopy*; Webb, G. A., Ed.; Academic Press: London, 1981; Vol. 11A, pp 99–182.

(43) Sokolic, L.; Modric, N.; Poje, M. *Tet. Lett.* **1991**, 32, 7477–7480.